Unusual features in the persistent emission of the Rapid Burster

Lubin, L.M.; Lewin, W.H.G.; van Paradijs, J.A.; van der Klis, M.

DOI
10.1093/mnras/261.1.149

Publication date
1993

Document Version
Final published version

Published in
Monthly Notices of the Royal Astronomical Society

Mon. Not. R. Astron. Soc. **261,** 149–164 (1993)

Unusual features in the persistent emission of the Rapid Burster

Lori M. Lubin,[1] Walter H. G. Lewin,[2] Jan van Paradijs[3] and Michiel van der Klis[3]

[1] *Princeton University Observatory, Peyton Hall, Princeton, NJ 08544-1001, USA*
[2] *Center for Space Research and Department of Physics, Massachusetts Institute of Technology, Room 37-627, Cambridge, MA 02139, USA*
[3] *Astronomical Institute 'Anton Pannekoek', University of Amsterdam, Center for High-Energy Astrophysics, Kruislaan 409, 1098 SJ Amsterdam, The Netherlands*

Accepted 1992 August 28. Received 1992 August 25; in original form 1992 May 11

ABSTRACT

We report the discovery of several distinct features in the persistent X-ray emission after long (> 30 s) type II bursts from the Rapid Burster. In 1985 August the persistent emission after type II bursts with integrated fluxes less than $\sim 4.8 \times 10^{-6}$ erg cm^{-2} exhibited (in 62 of 84 cases) a specific pattern characterized by a 'hump' in the early portion of the emission; this hump (which typically lasts ~200 s) is almost never observed after bursts with fluences greater than this value. For bursts with fluences a factor of 3 lower, the hump in the persistent emission following the burst is not seen when the time interval to the next burst becomes less than ~400 s. The emission during the hump is always harder than the average persistent emission. Quasi-periodic oscillations (QPO) with frequencies of ~40 mHz which were observed in 10 cases exclusively occur during a hump. In the 13 cases for which QPO of much higher frequency (~2–4 Hz) were observed, their frequencies were always ~4 Hz during the hump.

The persistent emission also exhibited 10 examples of sharp 'glitches' and 21 examples of small 'bumps' (lasting ~20–100 s). The glitches always occurred at approximately the same phase in the intervals between bursts. In seven cases the glitches were followed by a bump; in three of these cases the bump maximum occurred at almost exactly the same time (from 257–275 s) after the glitch.

We also present data on a type II burst observed during the dip in the persistent emission just prior to a burst. Our data show that this dip in the persistent emission is not the result of an obscuration of the source.

Key words: binaries: close – stars: individual: Rapid Burster – X-rays: bursts – X-rays: stars.

1 INTRODUCTION

The Rapid Burster (MXB 1730 − 335) was discovered in 1976 by Lewin et al. (1976). The source is located in the globular cluster Liller I (Liller 1977) at a distance of ~10 kpc (Kleinmann, Kleinmann & Wright 1976). The Rapid Burster distinguishes itself from other low-mass X-ray binaries by producing two types of X-ray burst (Hoffman, Marshall & Lewin 1978): type I bursts which are due to thermonuclear flashes on the surface of an accreting neutron star and type II bursts which are the result of accretion instabilities (gravitational potential energy). The behaviour of the type II bursts can be described as that of a relaxation oscillator; the integrated flux (E) in a burst is roughly proportional to the time interval (Δt) between it and the following burst (Lewin et al. 1976; Lewin 1977; White et al. 1978; Marshall et al. 1979; Inoue et al. 1980). For a detailed review, see Lewin, Van Paradijs & Taam (in preparation).

The Rapid Burster exhibits a variety of modes. At times only type II bursts are observed, with persistent X-ray emission after long (> 30 s) type II bursts. This persistent emission emerges gradually after a long type II burst and dips down before the occurrence of the next type II burst; this phenomenon is referred to as the 'dips' in the persistent emission (Marshall et al. 1979; Van Paradijs, Cominsky & Lewin 1979; Stella et al. 1988a). Type I bursts have also been observed in concurrence with type II bursts (Hoffman et al. 1978; Marshall et al. 1979; Kunieda et al. 1984a,b; Kawai

1985; Barr et al. 1987; Kawai et al. 1990) or solely with strong persistent emission (Kunieda et al. 1984b; Lewin 1985; Barr et al. 1987).

Quasi-periodic oscillations (QPO) of frequency ~2 Hz were discovered in two out of 63 long type II bursts by Tawara et al. (1982). Later, a complex QPO behaviour (of ~2–7 Hz) was discovered during type II bursts of ~10 to 680 s and during the persistent emission observed after long (>30 s) type II bursts (Stella et al. 1988a,b; Lubin et al. 1992; see also Lewin, Van Paradijs & Van der Klis 1988). In addition, Lubin et al. (1992) reported very strong oscillations with frequencies of ~40 mHz; the frequency gradually increased by ~3–50 per cent over a time-scale of ~100 s.

In this paper we present several new features in the persistent emission observed after long type II bursts.

2 THE OBSERVATIONS

In 1985 the Rapid Burster was observed with the Medium Energy (ME) detector array (Turner, Smith & Zimmermann

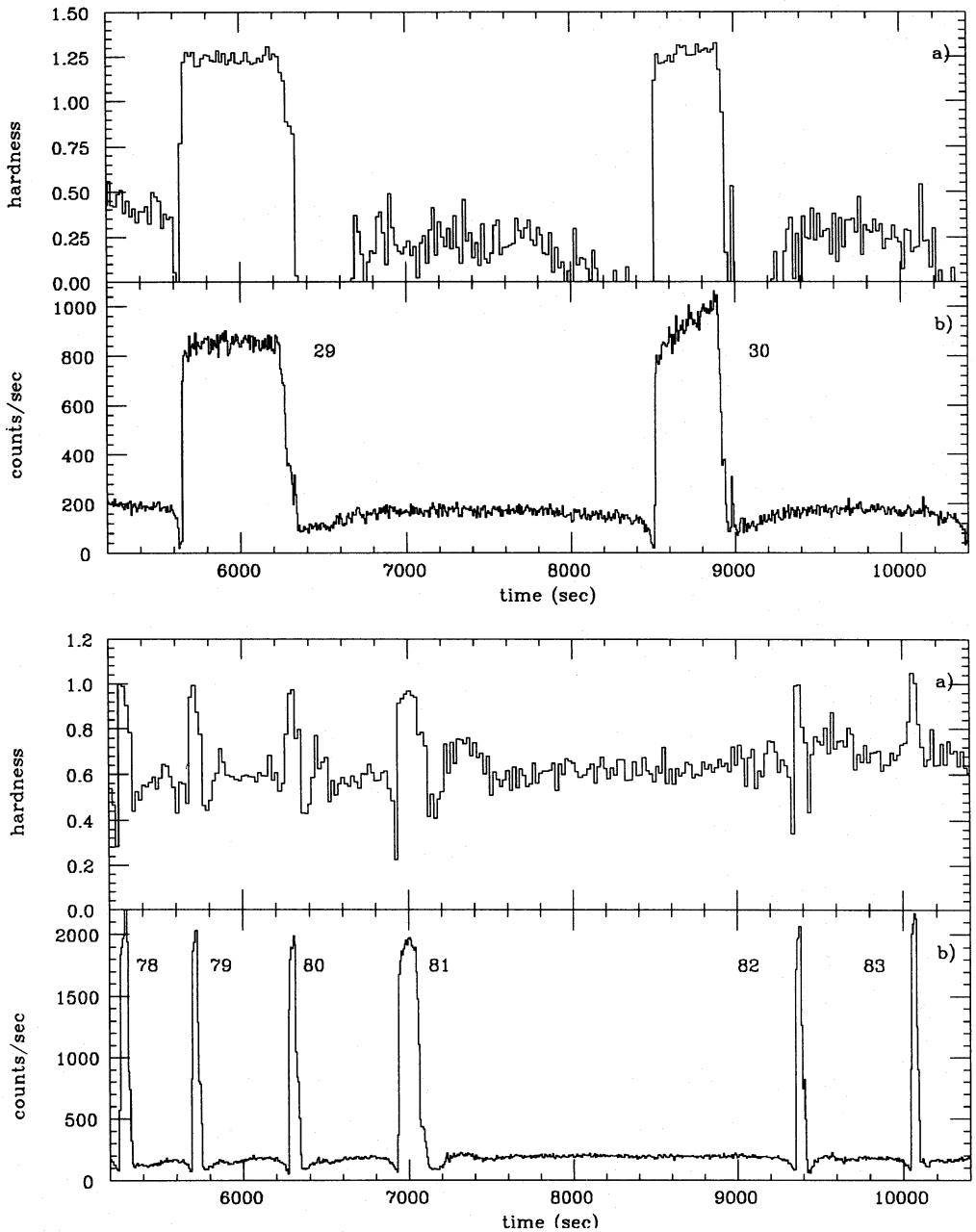

Figure 1. The hardness ratio (5–15/1–5 keV) versus time (a) and the corresponding light curve (b) of data from 1985 August 28 (bottom) and August 31 (top). The early portions of the persistent emission following bursts 79–82 are clearly *harder* (panel a) than the later persistent emission and correspond to a noticeable hump in the persistent emission profile (panel b). Bursts 29, 30, 78 and 83 do not show this characteristic hump nor the corresponding hardness. Notice the sharp feature immediately following burst 30; this phenomenon is referred to as a 'bump' in the persistent emission (see Section 4). All bursts are numbered in accordance with the convention of Stella et al. (1988a) and Lubin et al. (1992). The counting rates have been normalized to seven-eighths of the full array and corrected for detector transmission. The X-ray background (~150 count s^{-1}) has been subtracted.

1981) of *EXOSAT* on four occasions. We concentrate on the two observations (1985 August 28–29 and 30–31) during which the source emitted bursts with durations greater than 30 s and exhibited strong persistent emission.

2.1 1985 August 28–29

During the first 2.3 h (with the exception of a 15-min period; see Stella et al. 1988a) the transmission efficiencies (referenced to the full detector array) for the Rapid Burster and the nearby source 4U/MXB 1728−34 were ~41 and ~100 per cent, respectively. After UT 17:45, 1728−34 was excluded from the field of view (FOV) and the transmission efficiency for the Rapid Burster was 48 per cent. The persistent emission was highly variable. Strong ~2–4 Hz (and occasionally ~0.4–1.0 Hz) QPO were observed in the persistent emission as well as ~2–5 Hz QPO in the type II bursts. Background (off-source) data were taken from August 28 UT 14:14–15:29. Between August 29 UT 1:00 and 9:35 (the end of the observation), one-half of the detector array malfunctioned, producing an artificial flaring phenomenon. Some data taken during this period could not be fully analysed. A total of 40 type II bursts were seen during the observation. For details on the burst and general persistent emission characteristics, see table 1 of Tan et al. (1991).

2.2 1985 August 30–31

Between August 30 UT 18:28 and August 31 UT 00:10 and between August 31 UT 02:24 and 07:33, both half-arrays were pointing in the same direction, and the Rapid Burster was observed with a transmission efficiency (referenced to the full array) of ~46 per cent; 1728−34 was not in the FOV. Background (off-source) data were taken from August 30 UT 17:08–18:28 and from August 31 UT 07:33–08:28. In addition, one half-array was pointed at the background (off-source) between August 31 UT 00:10 and 01:10; the other half was off-source between August 31 UT 01:10 and 02:24. A total of 55 type II bursts were seen during this observation. For some details on the burst and general persistent emission characteristics of this observation, see table 1 of Tan et al. (1991).

3 A DISTINCTIVE PATTERN IN THE PERSISTENT EMISSION

During the 1985 August observations, the Rapid Burster emitted 95 type II bursts which were all followed by strong persistent emission. (The emission following 11 of the bursts could not be analysed due to transmission difficulties and contamination by the nearby source 1728−34.) Fig. 1(b) shows the light curve of data from 1985 August 28 and 31. The persistent emission which follows bursts 79, 80, 81 and 82 clearly shows a noticeable 'hump' just after the dip in the persistent emission, but the persistent emission following bursts 29, 30, 78 and 83 *does not*. Fig. 1(a) shows the corresponding hardness ratios (5–15/1–5 keV). The hump is characterized by emission with a spectrum that is clearly *harder* than that of the remaining interval (see also fig. 2 of Stella et al. 1988a, fig. 1 of Stella et al. 1988b, and fig. 6 of Lubin et al. 1992). After this hump, the persistent emission assumes a relatively constant level (which occasionally rises) until the onset of the dip prior to the next type II burst. After bursts 29, 30, 78 and 83, no hump, or the characteristic hardness variation, is clearly observed.

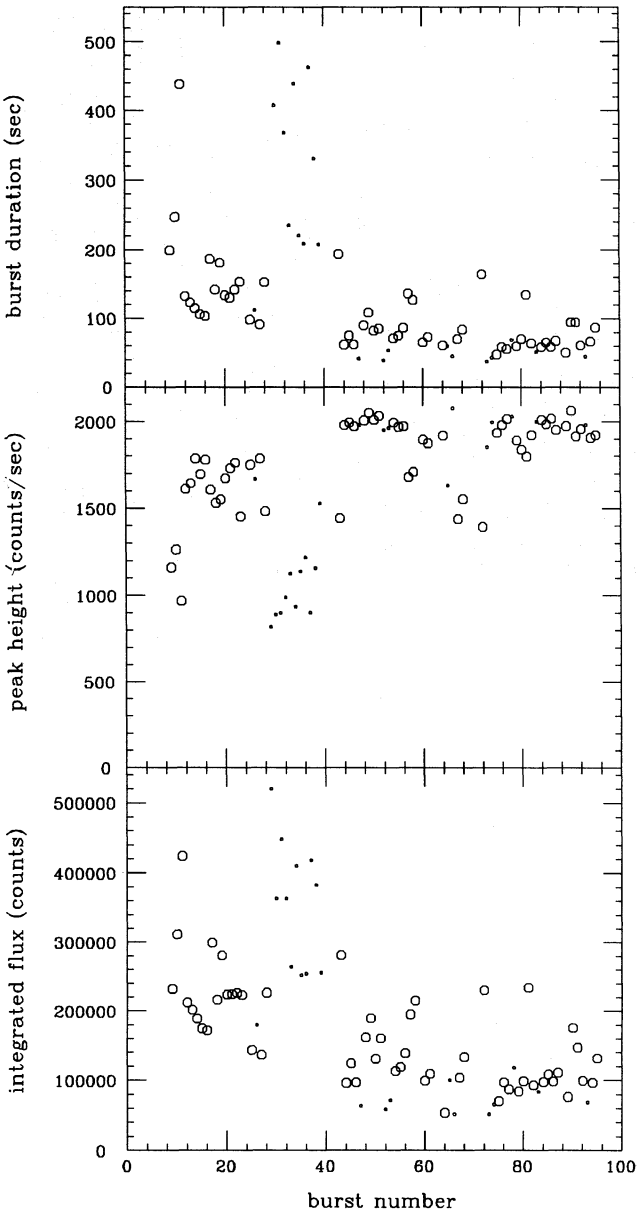

Figure 2. (a) Burst duration, (b) peak height and (c) integrated flux versus burst number. [All bursts are numbered according to the convention of Stella et al. (1988a) and Lubin et al. (1992).] 1 count is equivalent to $\sim 1.6\times10^{-11}$ erg cm^{-2} (bolometric). The bursts whose following persistent emission does and does not exhibit a hump are indicated with open circles and black dots, respectively. (For the determination of which persistent emission intervals exhibit a hump, see Section 3.) Based on our criteria, the hump is not observed in the persistent emission following bursts with integrated fluxes greater than $\sim 4.8\times10^{-6}$ erg cm^{-2} ($\sim 3\times10^{5}$ count) (e.g. bursts 29 and 30 of Fig. 1), though the exact fluence separation is not at all precise, since the persistent emissions following bursts both above and below this line do and do not exhibit humps (see Section 3). In addition, for 11 bursts of relatively low fluence (e.g. bursts 78 and 83 of Fig. 1), the hump is also *not* observed. However, for these bursts, the absence of a hump is not determined by the integrated flux of the burst but by the time interval to the following burst (see Fig. 3 and Section 3).

We have searched both observations and have classified each stretch of persistent emission as exhibiting a hump if the interval satisfies the following two criteria: (1) the characteristic hump (see Fig. 1) is clearly visible in the early portion (the first ~300 s) of the X-ray light curve, *and* (2) the hardness of this emission is $>4\,\sigma$ above the average hardness of the interval. In Fig. 2, we plot the duration, peak height and integrated flux of a burst versus burst number. [All bursts are numbered according to the convention of Stella et al. (1988a) and Lubin et al. (1992).] Those bursts whose following persistent emission exhibits a hump as defined above are indicated with circles; those whose persistent emission does not show a hump are indicated with black dots. Based on our criteria, the hump is usually not observed in the persistent emission following bursts with integrated fluxes greater than $\sim 4.8\times10^{-6}$ erg cm^{-2} ($\sim 3\times10^{5}$ count) (e.g. bursts 29 and 30 of Fig. 1). The exact fluence separation is not at all precise, as the persistent emissions following two bursts with fluences greater than this value do show humps, while the persistent emissions following five bursts with fluences in the range ~ 3.2–4.8×10^{-6} erg cm^{-2} (~ 2–3×10^{5} count) do not show humps. For the persistent emission following these relatively high-fluence bursts, it is also possible that the absence of a hump is dependent on the time of the observation, as all but two of the persistent emission stretches following bursts 25–40 do not show humps (see Fig. 2c). All of these bursts (and the following persistent emissions) occur between August 28 UT 23:56 and August 29 UT 07:57.

In addition, for 11 bursts of relatively low fluence [less than $\sim 1.6\times10^{-6}$ erg cm^{-2} ($\sim 10^{5}$ count)], the hump is also *not* observed (see Fig. 2c). For these relatively weak bursts, the absence of a hump is determined by the time interval to the next burst, rather than by the integrated flux in the burst (or time of the observation). Fig. 3 shows the relation between the integrated burst counts and the time interval to the next burst. The large open circles indicate those bursts whose following persistent emission does exhibit a hump. Fig. 3 shows that the time interval, and not the burst fluence, is the determining factor; when the time interval is less than ~400 s, no hump is observed (e.g. bursts 78 and 83 of Fig. 1).

3.1 The duration of the hump

We have investigated the possibility that the duration of the hump in the persistent emission is related to burst properties. The start of the hump was defined as the first 10-s time bin

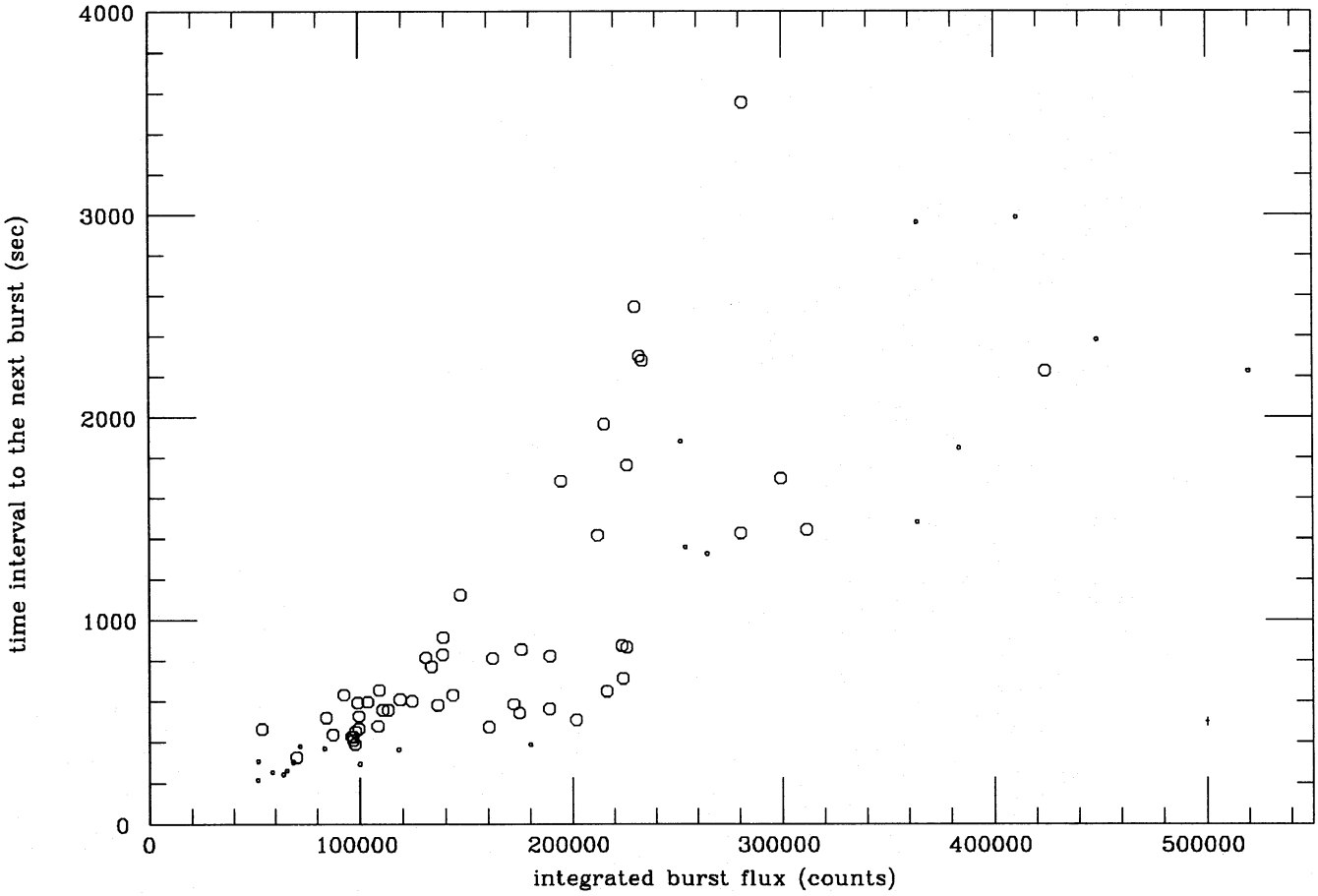

Figure 3. The waiting time to the next burst versus the integrated burst flux (counts). [1 count is equivalent to $\sim 1.6\times10^{-11}$ erg cm^{-2} (bolometric).] The large and small open circles respectively indicate the bursts whose following persistent emission does and does not show a hump. (For the criteria of determining which persistent emission intervals exhibit a hump, see Section 3.) In the 11 cases for which a relatively low-fluence burst is not followed by a hump, the absence is not uniquely determined by the integrated flux in the burst, but rather by the time interval to the following burst. If this interval is less than ~400 s, a hump and its associated spectral hardness (see Fig. 1 and Section 3) are not observed. A sample error bar is given in the lower right-hand corner.

which had a count rate greater than 90 per cent of the average level of the persistent emission (taken over the full interval until the next burst, excluding dips). The end of the hump was determined through a running average of 30 s (three 10-s time bins) starting at the 10-s time bin which contained the maximum count rate in the hump. The end of the hump was then defined as the central 10-s bin of the first running average whose value did not decrease by more than 2 σ over the previous average.

In Fig. 4 we plot the duration of the hump versus the peak height, integrated flux and duration of the previous burst, as well as the interval from the previous burst to the following burst. (Some bursts are not included due to uncertainties in transmission during the observations and the contamination of the nearby source 1728 − 34.) There is no obvious correlation between the duration, peak height and integrated flux of a burst and the duration of the hump; however, there may be some correlation between the time interval to the next burst and the duration of the hump for persistent emission intervals less than ~ 1000 s.

3.2 Unique properties of the emission during the hump

The hump in the persistent emission distinguishes itself through its profile in the X-ray light curve and its hardness (see Fig. 1 and above). The hump in the early portion of

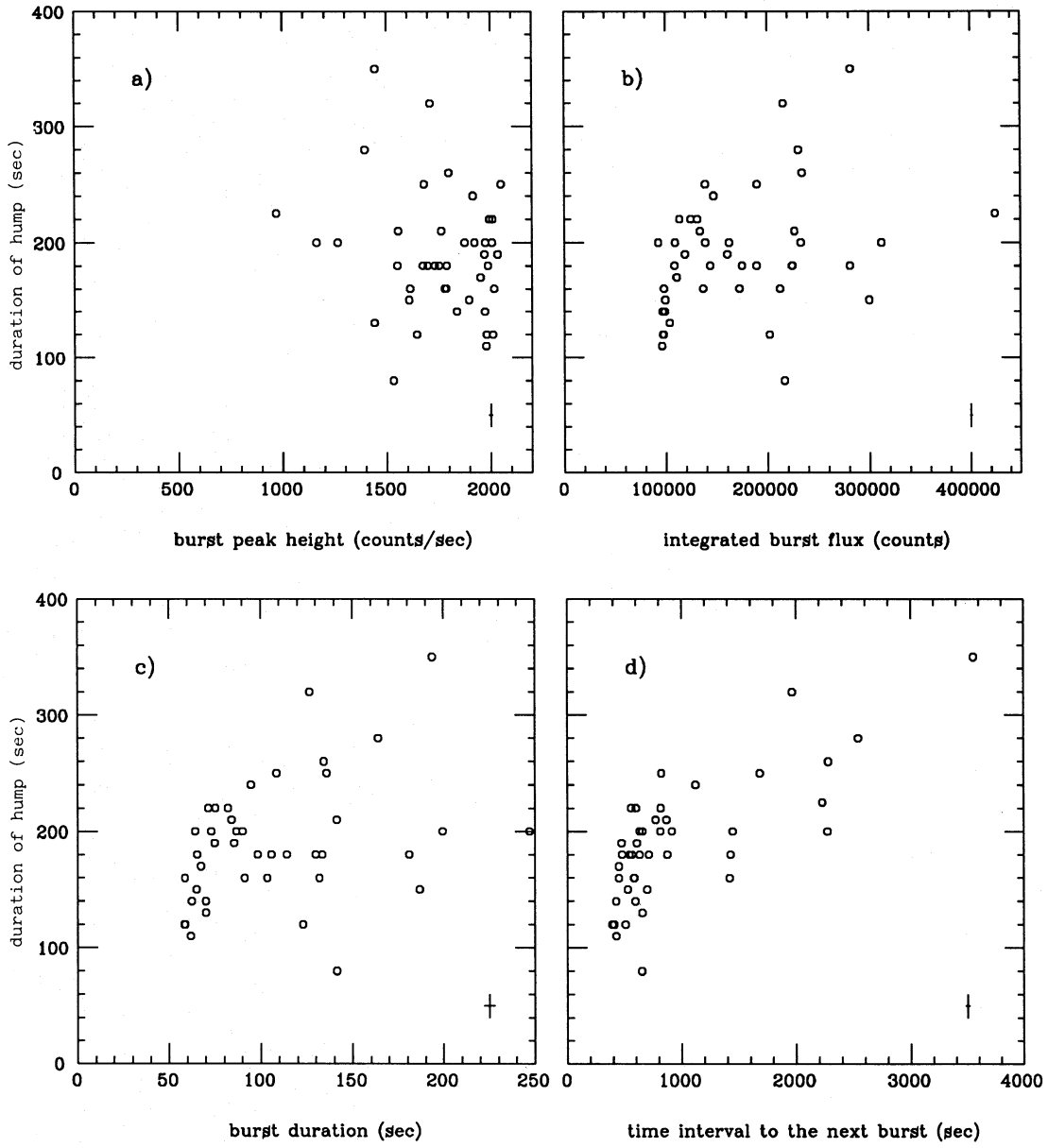

Figure 4. The duration of the hump (when observed) versus (a) the peak height, (b) the integrated flux, (c) the duration of the previous burst (see Section 3.1) and (d) the time interval to the next burst. [1 count is equivalent to $\sim 1.6 \times 10^{-11}$ erg cm^{-2} (bolometric).] There is no obvious correlation between the duration of the hump and the peak height, integrated flux or duration of the previous burst; however, there is apparently a correlation between the hump duration and the duration of the persistent emission interval for waiting times less than ~ 1000 s. Sample error bars are given in the lower right-hand corner of each panel.

the persistent emission is also related to the presence of oscillations in the X-ray emission.

Stella et al. (1988a) found that QPO were present in the persistent emission between some of the relatively short bursts with high peak luminosities (but modest fluence). In contrast, between the less luminous but very energetic and long bursts, QPO were never seen, even though the levels of persistent emission were similar. The QPO frequency in most cases decreased roughly from ~4 Hz shortly after a burst to ~2 Hz just prior to the next burst (see Stella et al. 1988a). When the ~4-Hz QPO are observed, they *always* occur during the hump in the persistent emission.

Lubin et al. (1992) reported very strong oscillations with frequencies of ~40 mHz (the frequency gradually increased by ~30–50 per cent over a time-scale of ~100 s) which were clearly visible in the raw X-ray light curves. They were often simultaneously observed with the ~4-Hz QPO. We have found that these oscillations were also *only* detected during the hump.

The connections of the QPO and the ~40-mHz oscillations with the hump do not necessarily mean that the properties are uniquely related. The probability that this is a result of a chance coincidence is not negligible (see Section 6).

4 SHARP GLITCHES AND SMALL BUMPS DURING THE PERSISTENT EMISSION

The Rapid Burster revealed two other characteristic properties of the persistent emission between type II bursts: a sharp 'glitch' and an enhancement in the persistent emission, hereafter referred to as a 'bump' (see Fig. 5). In the two 1985 August observations, we find a total of 10 sharp glitches and 21 bumps. Nine of the bumps occurred in the dip which immediately follows a burst (one of these cases shows a double bump). The other 12 bumps occurred at different locations later in the emission interval when the persistent emission had reached an approximately constant level. The sharp glitches always occur *just* after the persistent emission has come out of the dip following a burst. [Two of the glitches and two of the bumps cannot be accurately analysed due to the faulty detector on 1985 August 29 (see Section 2).] Fig. 5 shows examples of the sharp glitch and the small bump at both of the positions described above.

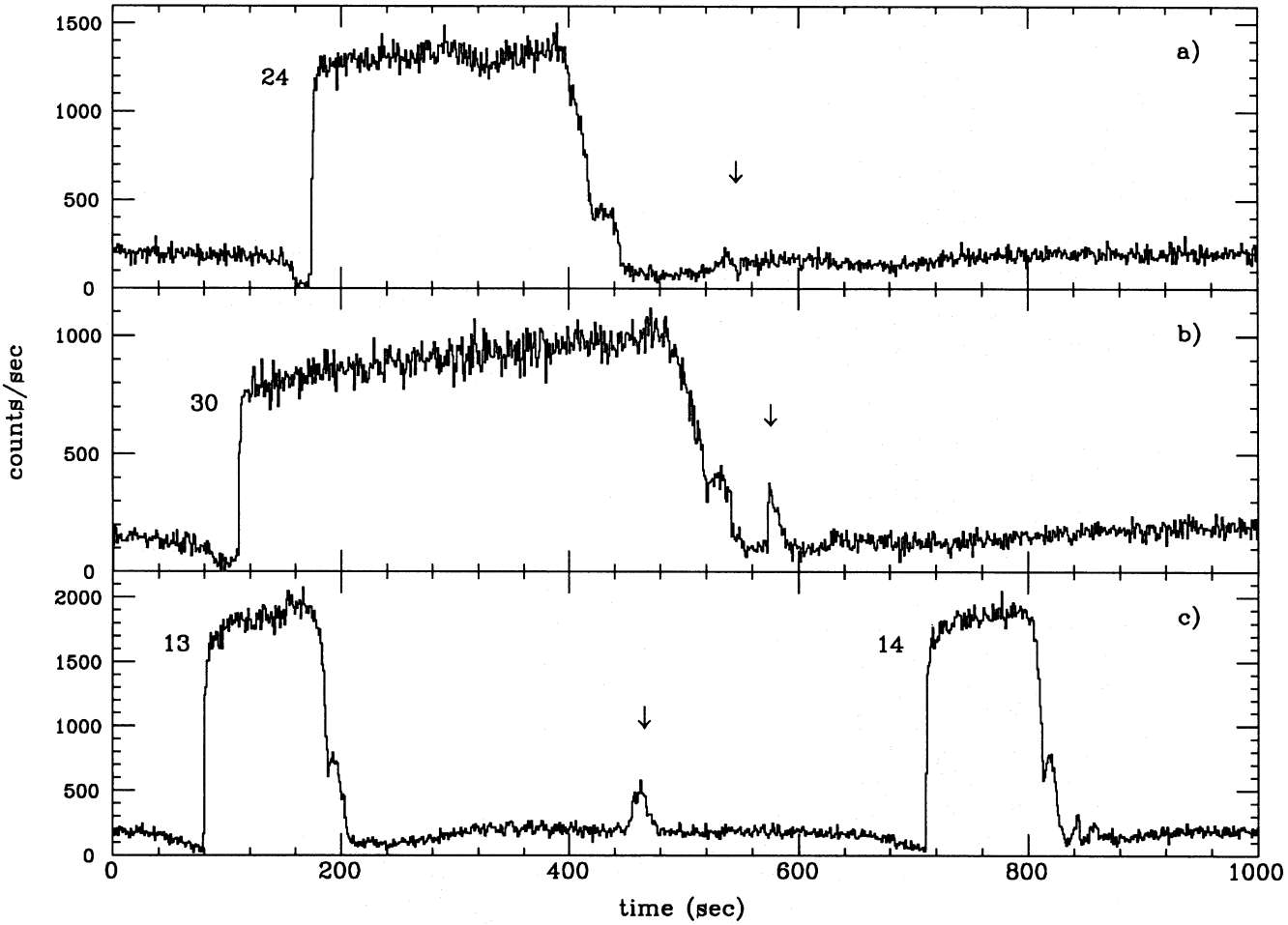

Figure 5. Examples of the sharp glitch (panel a) and the bumps (panels b, c) in the persistent emission between long type II bursts. The sharp glitches always occur soon after the persistent emission has come out of the dip following a burst (a). The bumps occur either in the dip which immediately follows a burst (b) or later in the emission interval (c). Arrows indicate the features. The numbers of the bursts are indicated. Notice the case of the double bump (see Section 4) which immediately follows burst 14. The counting rates have been normalized to seven-eighths of the full array and corrected for detector transmission. The background counting rate has been subtracted.

When a sharp glitch was observed in the persistent emission, it was preferentially *followed* by a small bump. This phenomenon was seen in seven out of a total of 10 cases of glitches. Fig. 6 shows five of these seven examples (the other two occurred on August 28 when the detector malfunctioned, superimposing artificial flaring on the source emission; see Section 2). In three of these cases, the bump maximum occurred between 257 and 275 s after the glitch (Fig. 6a–c).

4.1 Position of the glitches and bumps in the persistent emission

Fig. 7 is a histogram of the positions of the sharp glitches and the small bumps relative to the end of the previous type II burst. Panels (a) show the number of events versus the 'phase' in the interval, where the end of the previous burst and the beginning of the following burst are defined as 0 and 1, respectively. Panels (b) show the number versus the absolute

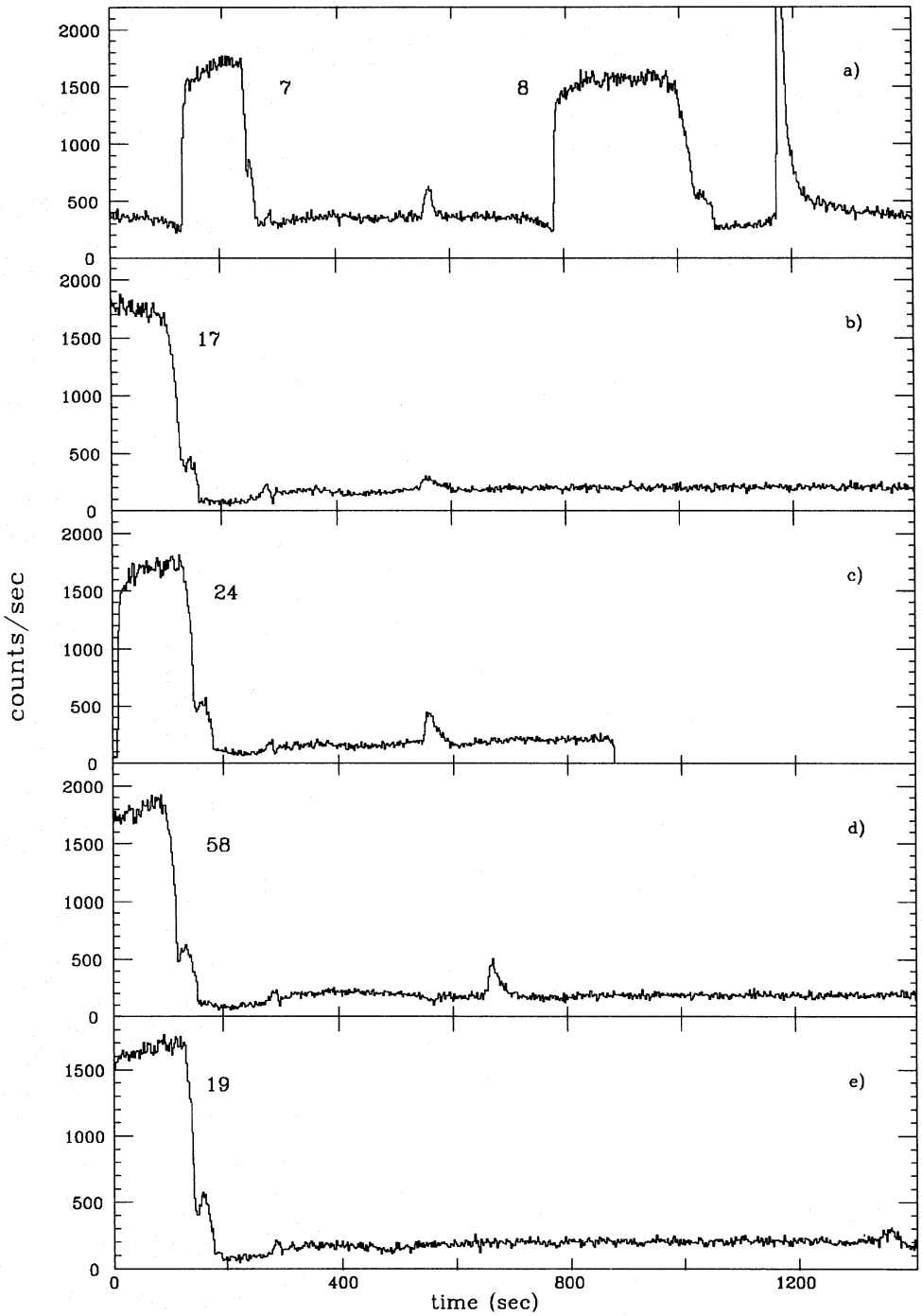

Figure 6. Five of the seven cases where the persistent emission between two bursts shows a sharp glitch followed by a bump. (Two cases are not shown because they occurred on August 28 when the detector malfunctioned; see Section 2.) In three cases (panels a,b,c) the bump maximum occurs between 257 and 275 s after the glitch. The burst numbers are indicated. Notice the type I burst in (a) which is from the nearby source 1728 − 34. The counting rates have been normalized to seven-eighths of the full array and corrected for detector transmission. The background counting rate has been subtracted.

time (in s) from the end of the previous burst. All the glitches cluster around a phase of 0.08 which corresponds to an absolute time of ~100 s. Nine of the bumps occurred immediately following the burst and the other bumps occurred at various positions later in the persistent emission interval.

4.2 Occurrence of the glitches and bumps

4.2.1 Time of the observation

The occurrence of the 10 glitches and 21 bumps appears to be uncorrelated with time during the two observations. Six of the glitches occurred on August 28, two on August 29, one on August 30 and one on August 31. Ten of the bumps occurred on August 28, three on August 29, two on August 30 and six on August 31.

4.2.2 Relation to burst properties

We have investigated the possibility that the occurrence of these glitches and bumps is related to properties of the previous burst. A total of 95 type II bursts were observed during the observations. In Fig. 8 we plot the duration, peak height and integrated flux of a burst versus burst number. The bursts which are followed by a stretch of persistent emission that exhibits *only* a sharp glitch are indicated by squares; a sharp glitch *and* a bump by diamonds; *only* a bump which immediately follows the burst by crosses; and *only* a bump in the middle of the persistent emission by squares. There does not appear to be a relation between the occurrence of the features and these burst properties.

In addition, the occurrence of the glitches and the bumps is not dependent on the spectral properties of the previous bursts. These bursts did not distinguish themselves from the

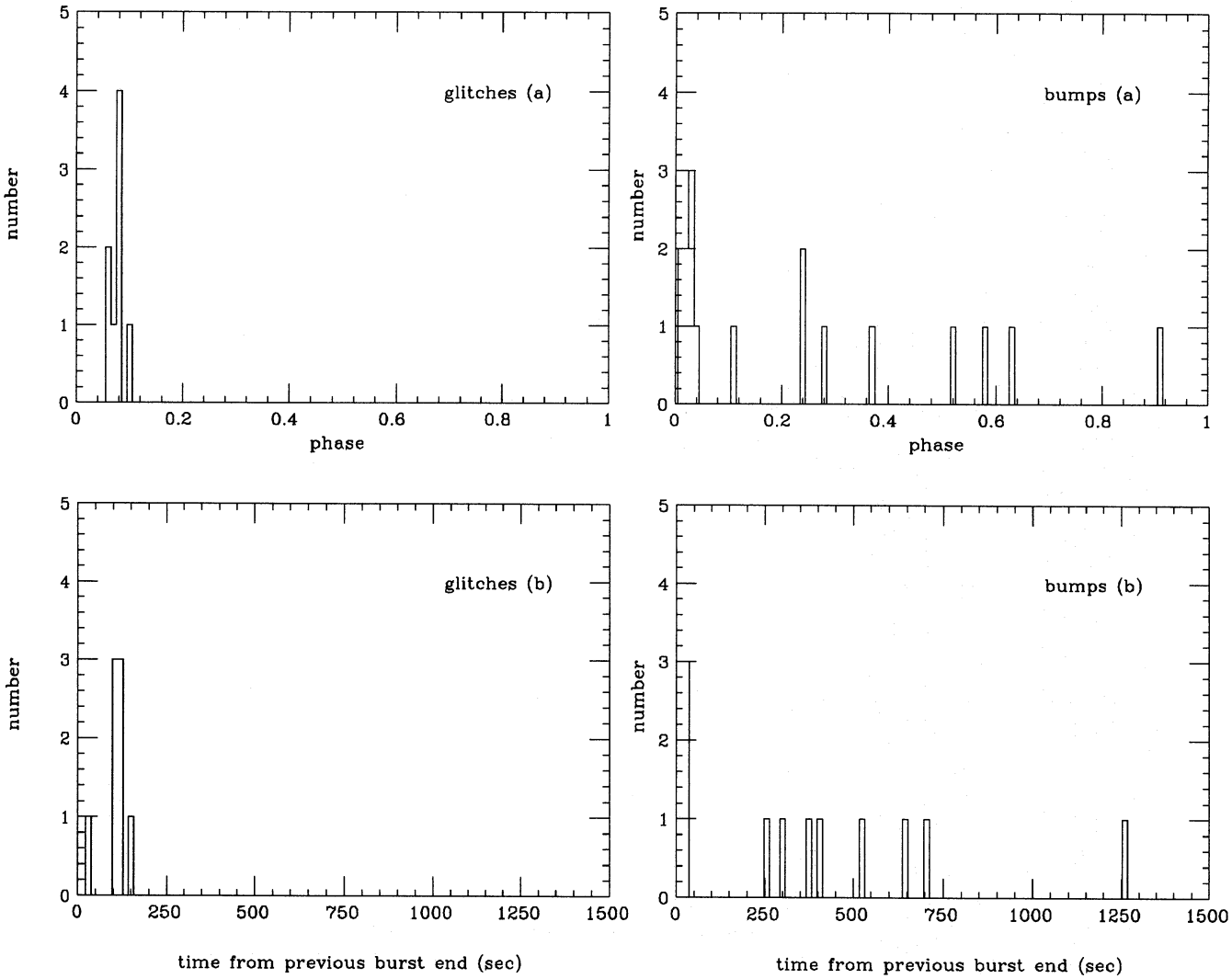

Figure 7. A histogram of the respective positions of the sharp glitches and the small bumps relative to the end of the previous type II burst. Panels (a) show the number of events versus the 'phase' in the persistent emission interval, where the end of the previous burst and the beginning of the following burst are defined as 0 and 1, respectively. Panels (b) show the number versus the absolute time (in s) from the end of the previous burst. All of the glitches cluster around a phase of 0.08 which corresponds to ~100 s. Nine of the bumps occur immediately following a burst and the other bumps occur at various positions later in the persistent emission interval.

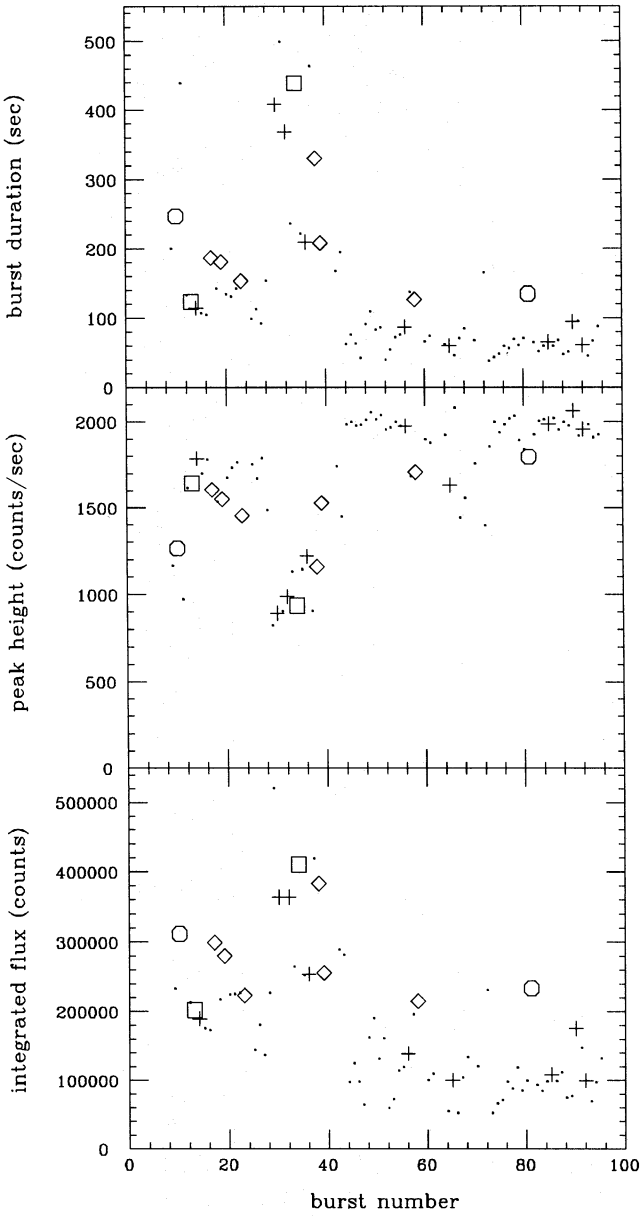

Figure 8. (a) Burst duration, (b) peak height and (c) integrated flux versus burst number. [All bursts are numbered according to the convention of Stella et al. (1988a) and Lubin et al. (1992).] The bursts which are followed by a stretch of persistent emission that exhibits *only* a sharp glitch are indicated by squares; a sharp glitch *and* a bump by diamonds; *only* a bump which immediately follows the burst by crosses; and *only* a bump in the middle of the persistent emission by squares. There is no obvious relation between the occurrence of the features and these burst properties. [1 count is equivalent to $\sim 1.6 \times 10^{-11}$ erg cm^{-2} (bolometric).]

other bursts by average spectral hardness (7.2–21.3/5.0–6.9 keV) or softness (2.9–4.7/0.9–2.6 keV) ratios, which ranged from 0.38–0.55 and 2.7–3.1, respectively.

4.2.3 *Relation to persistent emission*

Even though the hardness can change on short time-scales (see Fig. 1), the occurrence of the glitches and the bumps is not associated with these changes in hardness. Neither is the occurrence of these features related to the average intensity between two consecutive bursts of the persistent emission (background-subtracted), which remained approximately constant at $\sim 1.8 \times 10^{-9}$ erg cm^{-2} s^{-1} (230 count s^{-1}) during both observations and never deviated by more than ~ 20 per cent. There is no apparent connection between the occurrence of the hump and the glitches and bumps (see Section 6).

4.3 Profile and energy dependence of the glitches

4.3.1 *Composite profile*

All of the sharp glitches have almost exactly the same profile. They consist of a ~ 10–15 s period during which the emission is higher and a ~ 10–15 s period during which it is lower than the average persistent emission after the glitch. We have made a composite of the glitches by superimposing seven of the 10 cases. (The other three could not be used in the analysis due to the contribution of the nearby source 1728 − 34 and the faulty detector on August 28.) Fig. 9 is the composite glitch (in various energy ranges), where the individual glitches have been centred on the single 1-s time bin with the minimum count rate.

4.3.2 *Hardness of the composite profile*

In Fig. 10 we plot the variation of three hardness ratios in the composite glitch profile. The glitch is not obvious in the hardness plots.

4.4 Profile and energy dependence of the bumps

4.4.1 *Shapes of the bumps*

The bumps in both positions (at a phase < 0.04 and at all later phases; see Fig. 7) in the persistent emission (see Section 4.1) can be approximately characterized by two different shapes. They either appear triangular with a gradual rise and decay (13 cases) or exhibit a sharp rise and a gradual decay (eight cases) (see Figs 5b and c). The amplitude of the bump (above the average persistent emission level) varied from ~ 0.2–0.8×10^{-9} erg cm^{-2} s^{-1} (~ 20–100 count s^{-1}), and the duration varied in the range ~ 20–100 s.

4.4.2 *Energy evolution of the bumps*

Fig. 11 shows a light curve (in several energy ranges) of one of the 21 bumps, which is characteristic of the bumps in both positions (see Section 4.1), and its previous type II burst. The first three light curves look approximately the same.

4.4.3 *Hardness of the bumps*

In Fig. 12 we plot the same bump as shown in Fig. 11 for three hardness ratios. The type II burst exhibits no distinct softening (Hoffman et al. 1978). The bump has the same spectral hardness (within the uncertainties) as that of the persistent emission (and not that of the type II burst). To make a quantitative comparison, we have calculated hardness ratios (5–15/1–5 keV) by superimposing four cases of the bump, four ~ 150-s stretches of the persistent emission (which showed no features) and four type II bursts each with

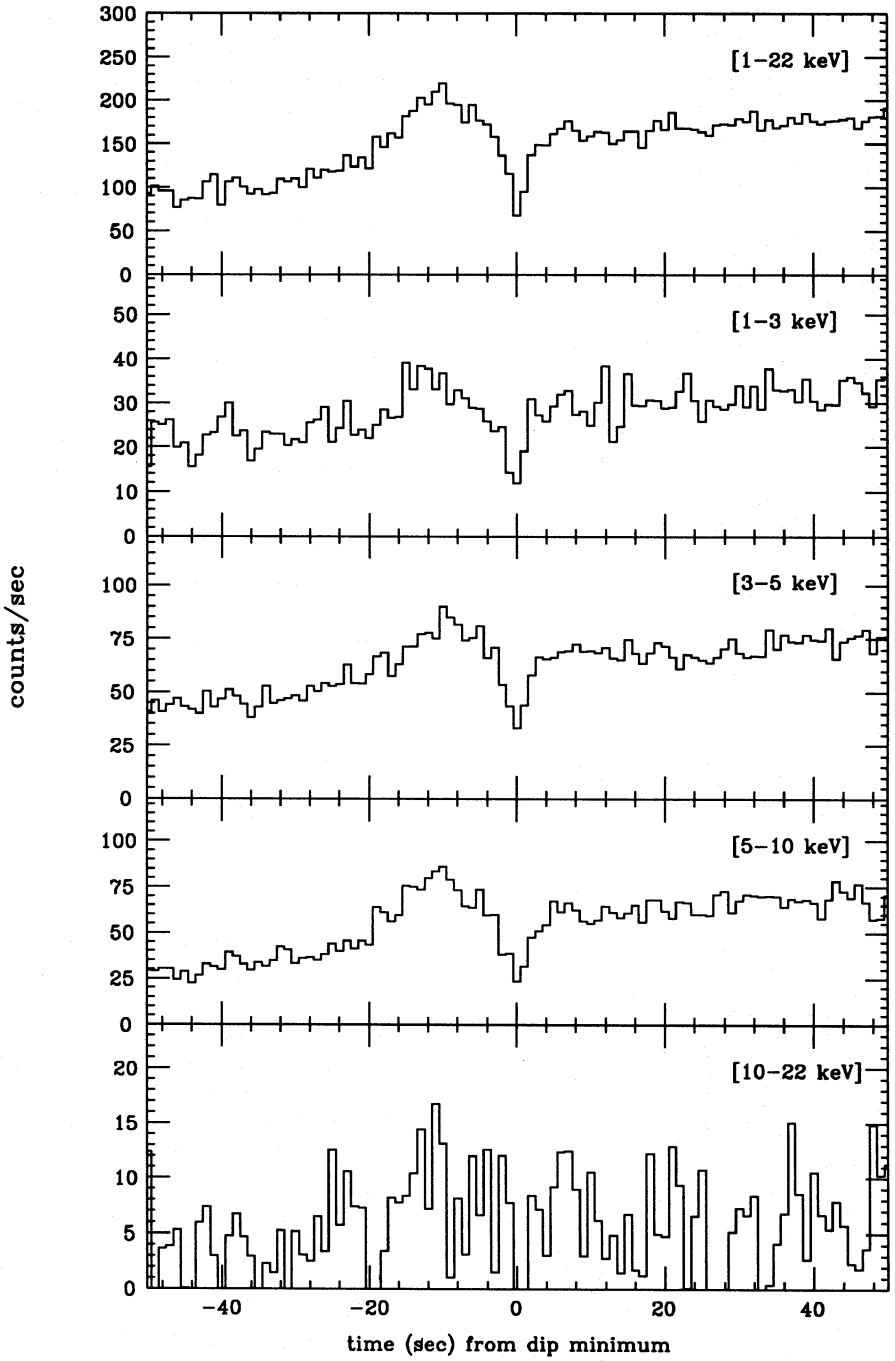

Figure 9. Composite profile of the sharp glitch in the persistent emission for various energy ranges. The composite is a superposition of seven of the 10 observed cases (see Section 4.3). The energy range of each panel is given in the upper right-hand corner. The counting rates have been normalized to seven-eighths of the full array and corrected for detector transmission. The background counting rate has been subtracted.

approximately the same peak flux. The hardness ratios are 0.59 ± 0.07, 0.69 ± 0.09 and 0.99 ± 0.03 for the composite of the bumps, persistent emission stretches and type II bursts, respectively. The hardness of the bump is consistent with that of the persistent emission, but not with that of the type II burst.

4.5 Power density spectra

To investigate these new features further, we have made a Fourier analysis using the high time resolution I5 (0.03125 s) and I7 (0.00391 s) data (see comments to table 1 of Lubin et al. 1992). Fast Fourier transforms (FFTs; normalized according to Leahy et al. 1983) were made of each of the features (27 FFTs in total). The consecutive data segments were 32 s long.

The power density spectra (PDS) do not show any distinct features, except the presence of a low-frequency noise component which is probably due to the trends of the features. The fractional rms variation of this low-frequency noise component (from 0.03 to 0.1 Hz) ranges from ~3 to ~21 per cent.

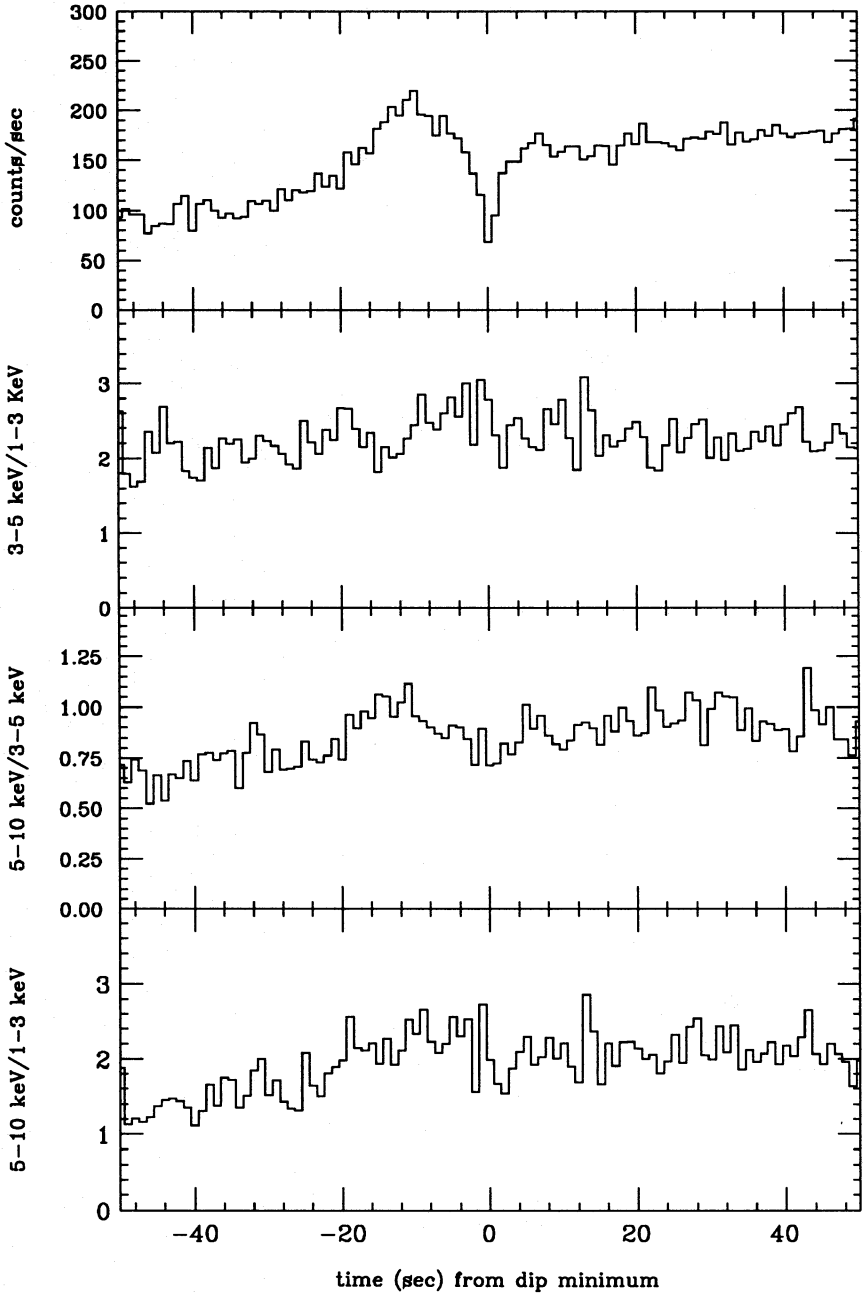

Figure 10. The composite glitch for three hardness ratios. (A light curve in the full 1–22 keV energy range is shown in the top panel.) The glitch is not distinguishable in the hardness plots.

5 A TYPE II BURST EMITTED DURING THE DIP IN THE PERSISTENT EMISSION

The persistent emission exhibits a distinct dip in emission after a long (> 30 s) type II burst and before the following burst (Marshall et al. 1979; Van Paradijs et al. 1979; Stella et al. 1988a). At August 30 UT 20:38 the Rapid Burster emitted a ~ 5-s burst in the dip in the persistent emission. The burst is clearly a type II burst as it shows no spectral evolution (Fig. 13) and has the same hardness ratios as does the following type II burst (Fig. 14). The hardness ratios in the 5.55–10.25/1–3.4 keV range are 0.52 ± 0.15, 1.03 ± 0.07 and 1.07 ± 0.11 for the persistent emission, the ~ 60-s type II burst and the burst in the dip, respectively. The hardness of the burst in the dip is consistent with that of the following ~ 60-s type II burst.

6 SUMMARY AND DISCUSSION

In 62 (out of 84) type II bursts, we observed a 'hump' in the persistent emission following the burst. In general, no hump was observed when either the preceding burst fluence was greater than $\sim 4.8 \times 10^{-6}$ erg cm^{-2}, or the time interval from the preceding to the following burst was less than ~ 400 s (Figs 2 and 3). The dividing line of burst fluence indicated in

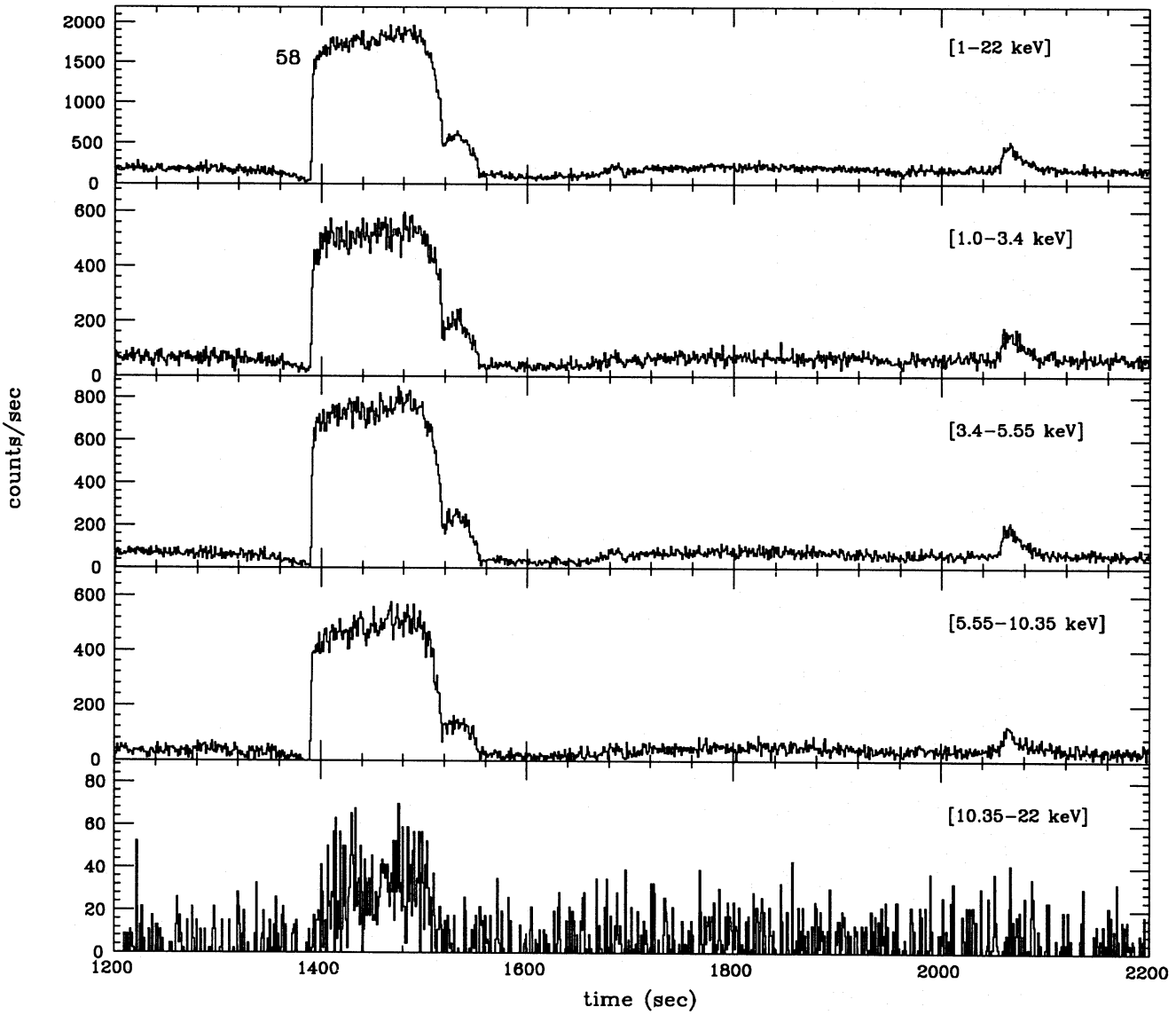

Figure 11. The evolution of one bump [and its previous type II burst (burst 58)] as a function of energy. The energy range of each panel is given in the upper right-hand corner. Notice the glitch at ~1700 s which is most visible in the 1–22 keV energy range. The counting rates have been normalized to seven-eighths of the full array and corrected for detector transmission. The background counting rate has been subtracted.

the latter case, however, is not at all precise, as the persistent emissions following two bursts with fluences greater than this value do show humps, while the persistent emissions following five bursts with fluences in the range $\sim 3.2\text{–}4.8 \times 10^{-6}$ erg cm^{-2} ($\sim 2\text{–}3 \times 10^5$ count) do not show humps. For the persistent emission following these relatively high-fluence bursts, it is also possible that the absence of a hump is dependent on the time of the observation, as all but two of the persistent emission stretches following bursts 25–40 do not show humps (see Fig. 2c). All of these bursts (and the following persistent emission) occurred between August 28 UT 23:56 and August 29 UT 07:57.

The humps are spectrally harder than the average persistent emission. They typically last ~200 s and occur exclusively in the early portion of the persistent emission immediately after the dip following the burst (Fig. 1). There appears to be a correlation between the duration of the hump and the time interval from the burst that precedes the hump to the next burst (Fig. 4d); no such correlation exists between the duration of the hump and the fluence of the preceding burst (Fig. 4b), even though there is a clear correlation between the burst fluence and the time interval to the next burst (see Introduction and Fig. 3). In our data, for a given burst fluence, the interval to the next burst can be predicted to an accuracy of ~35 per cent (standard deviation); for a given hump duration, the burst interval can be predicted to an accuracy of ~40 per cent (standard deviation).

In all 13 (out of 84) cases for which QPO are detected in the persistent emission (see Stella et al. 1988a; Lubin et al. 1992), the persistent emission exhibits a hump. [Since the centroid frequency of the QPO generally decreases from ~4 Hz shortly after a burst to ~2 Hz just before the next burst (Stella et al. 1988a), the QPO frequency during the hump is always ~4 Hz.] In 10 (out of 84) cases, strong oscillations

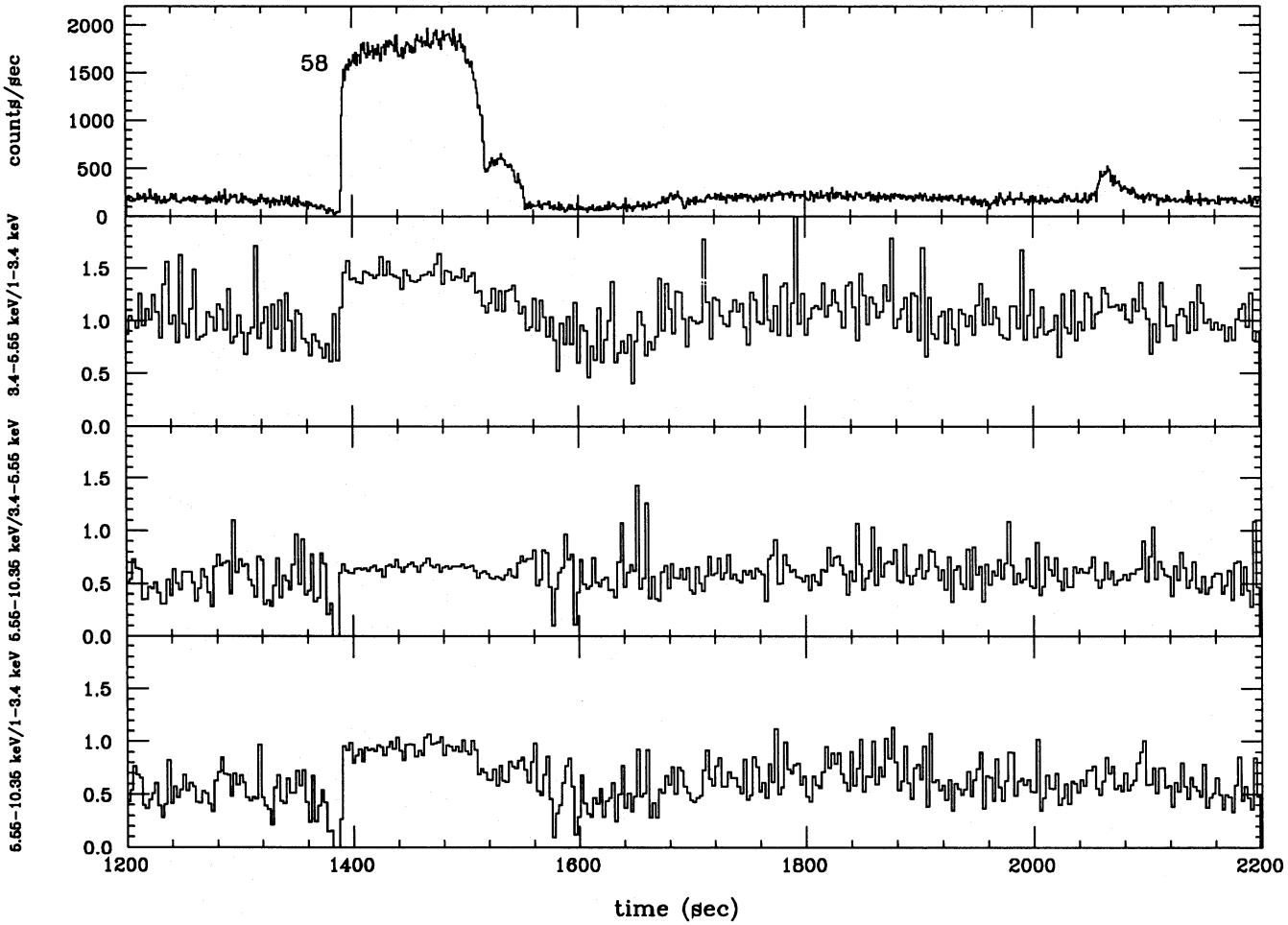

Figure 12. Three hardness ratios of the bump (from Fig. 11) and its previous type II burst (burst 58). (A light curve in the full 1–22 keV energy range is shown in the top panel.) The type II burst exhibits no distinct softening (Hoffman et al. 1978). The spectral hardness of the bump is the same (within the uncertainties) as that of the persistent emission (but not that of the type II burst) (see Section 4.4).

with a mean frequency of ~40 mHz were observed in the persistent emission (see Introduction; Lubin et al. 1992). These oscillations (which persisted for only ~100 s) always occurred in the portion of the persistent emission where humps occurred. In all 10 cases a hump was present.

Thus, whenever the ~4-Hz QPO or the ~40-mHz oscillations were observed, there was *always* a hump. This, however, does not necessarily mean that the occurrences of the QPO or the ~40-mHz oscillations are uniquely connected with the occurrence of a hump. Since the probability of observing a hump is 0.73 (62/84), the probabilities that a hump is observed accidentally in all 13 cases of QPO and in all 10 cases of ~40-mHz oscillations are ~2 and ~5 per cent, respectively. A connection between the QPO and the ~40-mHz oscillations, however, is not in question, as they were simultaneously detected in seven cases (Lubin et al. 1992).

A glitch with a characteristic profile was observed in 10 (out of 84) cases in the persistent emission near the end of the dip that follows a burst (Figs 5, 6, 8, 9 and 10). The occurrence of a glitch is not correlated with the fluence, peak flux or duration of the preceding burst (or the burst which follows). If we call the phase of the persistent emission 0 at the end of the preceding burst and 1 at the start of the burst that follows, all of the glitches occur in a narrow phase interval from 0.06 to 0.10 (Fig. 7a). Enhanced periods of persistent emission (referred to as bumps) which last ~20–100 s were observed in 21 cases (Figs 5, 6, 11 and 12). In nine cases, the bumps occurred before phase 0.05 (i.e. in the dip following a burst); in the remaining 11 cases, they did not occur at a preferred phase (Fig. 7a). The glitches are preferentially followed by a bump, as both a glitch and a bump were observed in the persistent emission between two consecutive bursts in seven (out of 10) cases. In three of these cases the bump maximum occurred almost exactly at the same time (257–275 s) after the glitch.

There is no connection between the glitches and the humps. In eight (out of 10) cases, a glitch was followed by a hump (Figs 5 and 6). (One would expect a mean of 7.3 out of 10 if the two were uncorrelated.)

No glitch was ever observed when the ~40-mHz oscillations were also detected. This does not mean that the occurrence of the glitches precludes the occurrence of these oscillations (and vice versa), as the probability of zero

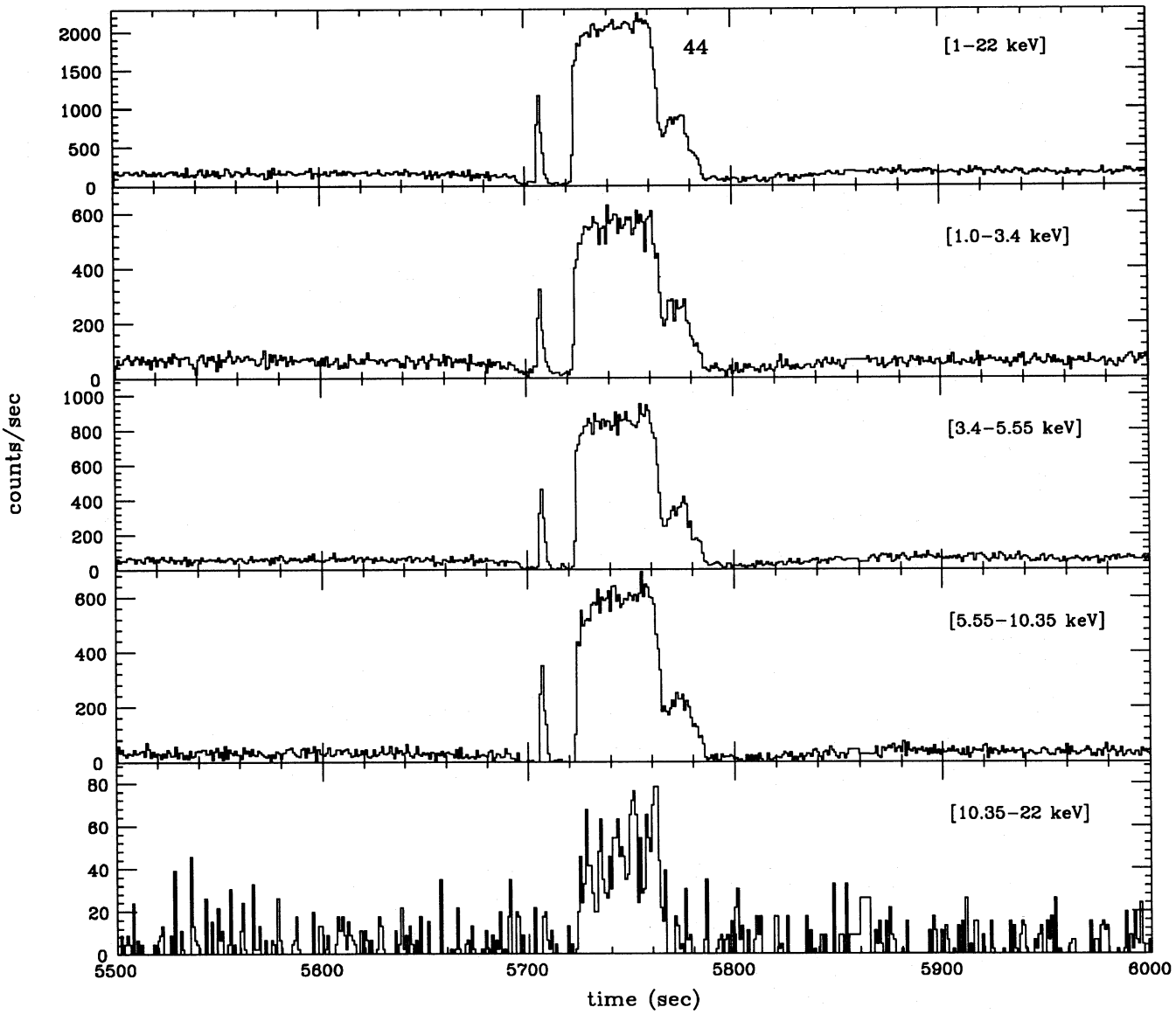

Figure 13. The spectral evolution of the type II burst emitted in the dip in the persistent emission just prior to a long (~60 s) type II burst (burst 44). The burst in the dip shows little spectral evolution (characteristic of type II bursts). The energy range of each panel is given in the upper right-hand corner. The counting rates have been normalized to seven-eighths of the full array and corrected for detector transmission. The background counting rate has been subtracted.

coincidence is ~28 per cent if the glitches and oscillations are unrelated. In addition, we would not be able to detect a glitch in the presence of strong oscillations.

One bump was observed just prior to the ~40-mHz oscillations. The probability of one random coincidence (the occurrence of both a bump and the oscillations between two consecutive bursts) is ~20 per cent. Thus there is no evidence that the bumps and the oscillations are related (as was the case for the glitches).

A type II burst was observed in a dip just prior to a burst (Figs 13 and 14). This demonstrates that this dip is not the result of obscuration.

We have shown in this paper that, during the 1985 August observations with *EXOSAT* when the burst durations varied from ~30 to 680 s, the persistent emission also exhibited distinct features such as humps, glitches and bumps, in addition to the dips reported previously (Marshall et al. 1979; Van Paradijs et al. 1979; Stella et al. 1988a). The humps occurred very often (~73 per cent of all cases), and the glitches and bumps occurred in ~12 and ~25 per cent of all cases, respectively. The origin of the persistent emission, which is exclusively and always observed after bursts longer than ~30 s, is not understood. It is, therefore, difficult to speculate on the origin of the above features in the persistent emission.

However, it is certain that the bumps which sometimes appear like small bursts (Fig. 5) are not produced by the same mechanism that produces the bursts; the spectra of the bumps are indistinguishable from that of the persistent emission and are very different from those of the bursts (Fig. 12).

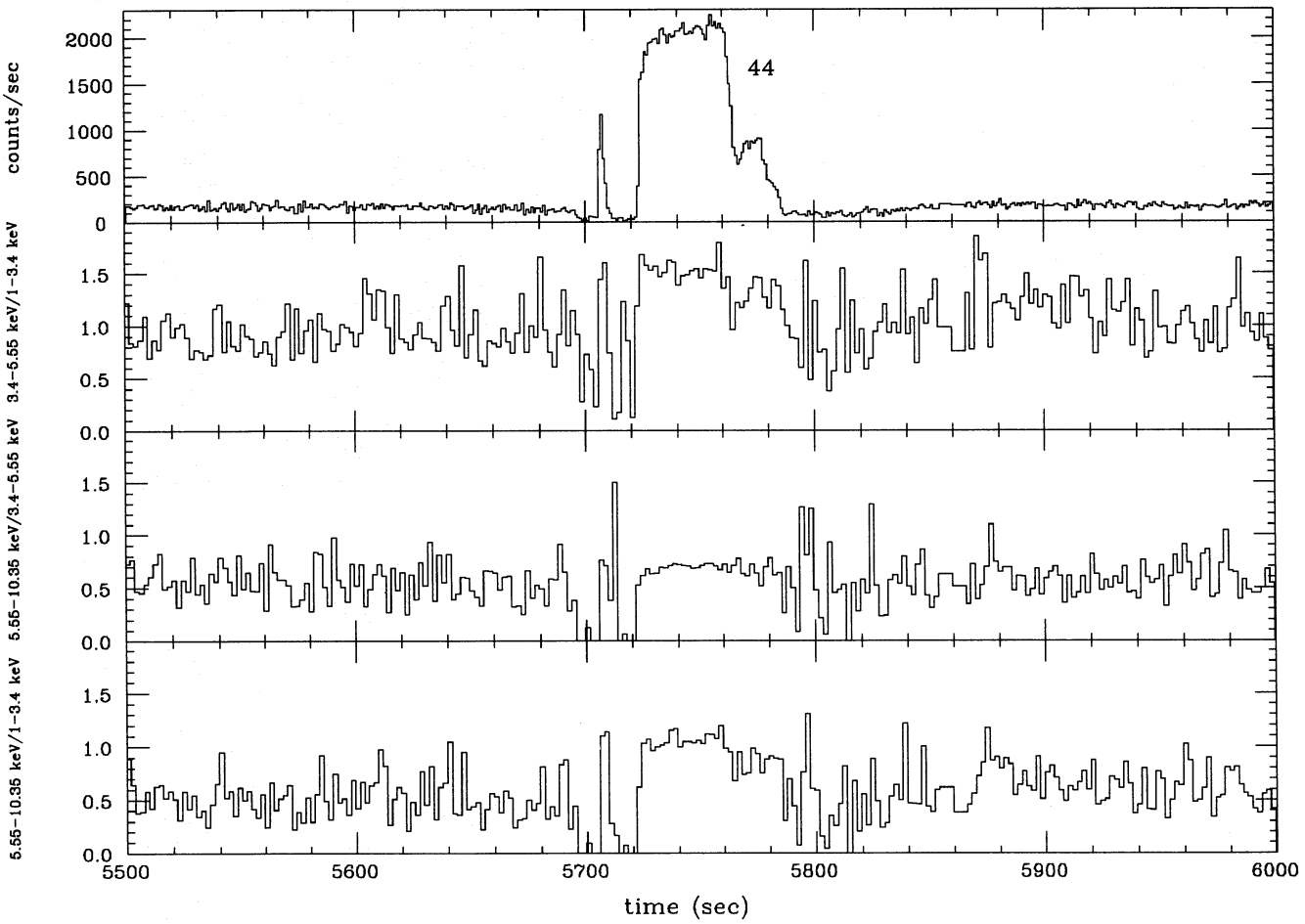

Figure 14. The burst in the dip and its following type II burst (burst 44) for three hardness ratios. (A light curve in the full 1–22 keV energy range is shown in the top panel.) The burst in the dip and the ~60-s type II burst have similar spectral hardnesses (within the uncertainties) (see Section 5).

The glitches (often accompanied by the occurrence of a bump during the same interval) have spectra which are also indistinguishable from that of the persistent emission (Fig. 10). They consist of a ~10–15 s period during which the emission is higher and a ~5–10 s period during which it is lower than the average persistent emission after a glitch (Fig. 9). The excess integrated flux during the period that the emission is higher is about equal to the 'missing' integrated flux during the period that the emission is lower. This seems to indicate that, after a burst when the persistent emission level gradually increases (and thus presumably the accretion rate on to the neutron star), there can be an overshoot in the persistent emission (the accretion rate is 'too high') which in turn, as a compensation, causes the brief drop in the accretion.

The Rapid Burster exhibits many idiosyncrasies not present in *any* other known low-mass X-ray binary. The features reported here add to the mystery of the Rapid Burster.

ACKNOWLEDGMENTS

WHGL is supported by the United States National Aeronautics and Space Administration under grants NAG5-1723 and NAG8-700. JvP acknowledges support from NATO through grant RG 331/88. This paper is supported in part by the Netherlands Organization for Scientific Research (NWO) under grant PGS 78-277.

REFERENCES

Barr P., White N. E., Haberl F., Stella L., Pollard G., Gottwald M., Parmer A. N., 1987, A&A, 176, 69
Hoffman J. A., Marshall H. L., Lewin W. H. G., 1978, Nat, 271, 630
Inoue H. et al., 1980, Nat, 283, 358
Kawai N., 1985, PhD thesis, University of Tokyo (ISAS Res. Note 30)
Kawai N., Matsuoka M., Inoue H., Ogawara Y., Tanaka Y., Kunieda H., Tawara Y., 1990, PASJ, 92, 115
Kleinmann D. E., Kleinmann S. G., Wright E. L., 1976, ApJ, 210, L83
Kunieda H. et al., 1984a, PASJ, 35, 215
Kunieda H. et al., 1984b, PASJ, 36, 807
Leahy D. A., Darbro W., Elsner R. F., Weisskopf M. C., Sutherland P. G., Kahn S., Grindlay J. E., 1983, ApJ, 266, 160
Lewin W. H. G., 1977, Am. Sci., 65, No. 5, 605
Lewin W. H. G., 1985, in Tanaka Y., Lewin W. H. G., eds, Galactic and Extragalactic Compact X-ray Sources. Inst. Space Astronaut. Sci., Tokyo, p. 89
Lewin W. H. G. et al., 1976, ApJ, 207, L95
Lewin W. H. G., van Paradijs J., van der Klis M., 1988, Space Sci.

Rev., 46, 273
Liller W., 1977, ApJ, 213, L21
Lubin L. M., Stella L., Lewin W. H. G., Tan J., van Paradijs J., van der Klis M., Penninx W., 1991, MNRAS, 249, 300
Lubin L. M., Lewin W. H. G., Rutledge R. E., van Paradijs J., van der Klis M., Stella L., 1992, MNRAS, 258, 759
Marshall H. L., Ulmer M. P., Hoffman J. A., Doty J., Lewin W. H. G., 1979, ApJ, 227, 555
Stella L., Haberl F., Lewin W. H. G., Parmar A., White N. E., van Paradijs J., 1988a, ApJ, 324, 379
Stella L., Haberl F., Lewin W. H. G., Parmar A., van der Klis M., van Paradijs J., 1988b, ApJ, 327, L13
Tan J., Lewin W. H. G., Lubin L. M., van Paradijs J., Penninx W., van der Klis M., Damen E., Stella L., 1991, MNRAS, 251, 1
Tawara Y., Hayakawa S., Kunieda H., Makino F., Nagase F., 1982, Nat, 299, 38
Turner M. J. L., Smith A., Zimmermann H. U., 1981, Space Sci. Rev., 30, 513
van Paradijs J., Cominsky L., Lewin W. H. G., 1979, MNRAS, 189, 387
White N. E., Mason K. O., Carpenter G. F., Skinner G. K., 1978, MNRAS, 184, 1P